OPEN ACCESS

Original research

*HLA-DPA1*02:01~B1*01:01* is a risk haplotype for primary sclerosing cholangitis mediating activation of NKp44+ NK cells

Britta F Zecher ,[1,2] David Ellinghaus ,[3] Sebastian Schloer,[2] Annika Niehrs,[2] Benedetta Padoan,[2] Martin E Baumdick,[2] Yuko Yuki,[4] Maureen P Martin,[4] Dawid Glow,[5] Jennifer Schröder-Schwarz,[6] Jennifer Niersch,[2] Sébastien Brias,[1,2] Luisa M Müller,[2] Robin Habermann,[2] Paul Kretschmer,[2] Tristan Früh,[2] Janis Dänekas,[2] Malte H Wehmeyer,[1] Tobias Poch,[1] Marcial Sebode,[1] International PSC Study Group (IPSCSG),[7] Eva Ellinghaus,[3] Frauke Degenhardt,[3] Christian Körner,[2] Angelique Hoelzemer,[1,2] Boris Fehse ,[5] Karl J Oldhafer,[8] Udo Schumacher,[6] Guido Sauter,[9] Mary Carrington,[4,10] Andre Franke,[3] Madeleine J Bunders,[2,11] Christoph Schramm,[1,12] Marcus Altfeld [2,13]

► Additional supplemental material is published online only. To view, please visit the journal online (http://dx.doi.org/10.1136/gutjnl-2023-329524).

For numbered affiliations see end of article.

Correspondence to
Professor Marcus Altfeld, Leibniz Institute of Virology, Hamburg, Hamburg, Germany; marcus.altfeld@leibniz-liv.de

CS and MA are joint senior authors.

Received 17 January 2023
Accepted 11 September 2023

To cite: Zecher BF, Ellinghaus D, Schloer S, *et al*. *Gut* Epub ahead of print: [*please include* Day Month Year]. doi:10.1136/gutjnl-2023-329524

ABSTRACT

Objective Primary sclerosing cholangitis (PSC) is characterised by bile duct strictures and progressive liver disease, eventually requiring liver transplantation. Although the pathogenesis of PSC remains incompletely understood, strong associations with HLA-class II haplotypes have been described. As specific HLA-DP molecules can bind the activating NK-cell receptor NKp44, we investigated the role of HLA-DP/NKp44-interactions in PSC.

Design Liver tissue, intrahepatic and peripheral blood lymphocytes of individuals with PSC and control individuals were characterised using flow cytometry, immunohistochemical and immunofluorescence analyses. HLA-DPA1 and HLA-DPB1 imputation and association analyses were performed in 3408 individuals with PSC and 34 213 controls. NK cell activation on NKp44/HLA-DP interactions was assessed in vitro using plate-bound HLA-DP molecules and HLA-DPB wildtype versus knock-out human cholangiocyte organoids.

Results NKp44+NK cells were enriched in livers, and intrahepatic bile ducts of individuals with PSC showed higher expression of HLA-DP. HLA-DP haplotype analysis revealed a highly elevated PSC risk for *HLA-DPA1*02:01~B1*01:01* (OR 1.99, $p=6.7\times10^{-50}$). Primary NKp44+NK cells exhibited significantly higher degranulation in response to plate-bound HLA-DPA1*02:01-DPB1*01:01 compared with control HLA-DP molecules, which were inhibited by anti-NKp44-blocking. Human cholangiocyte organoids expressing HLA-DPA1*02:01-DPB1*01:01 after IFN-γ-exposure demonstrated significantly increased binding to NKp44-Fc constructs compared with unstimulated controls. Importantly, HLA-DPA1*02:01-DPB1*01:01-expressing organoids increased degranulation of NKp44+NK cells compared with HLA-DPB1-KO organoids.

Conclusion Our studies identify a novel PSC risk haplotype *HLA-DP A1*02:01~DPB1*01:01* and provide clinical and functional data implicating NKp44+NK cells that recognise HLA-DPA1*02:01-DPB1*01:01 expressed on cholangiocytes in PSC pathogenesis.

WHAT IS ALREADY KNOWN ON THIS TOPIC

⇒ NK cells have been implicated in the pathogenesis of primary sclerosing cholangitis (PSC); however, the molecular mechanisms mediating NK cell activation in PSC remain unknown.

WHAT THIS STUDY ADDS

⇒ This study identifies *HLA-DPA1*02:01~B1*01:01* as a risk haplotype for PSC and demonstrates that NKp44+NK cells can be activated via binding to HLA-DPA1*02:01-B1*01:01 molecules expressed by cholangiocytes.

HOW THIS STUDY MIGHT AFFECT RESEARCH, PRACTICE OR POLICY

⇒ Our results may initiate further studies to evaluate the potential of the NKp44/HLA-DP interaction as a target for an immunomodulatory therapy to attenuate disease progression.

INTRODUCTION

Primary sclerosing cholangitis (PSC) is an immune-mediated liver disease with increasing incidence affecting approximately 7–16 in 100 000 Europeans.[1] Chronic inflammation in PSC leads to scarring of intrahepatic and extrahepatic bile ducts.[2] Consequently, people with PSC develop progressive liver disease, eventually requiring liver transplantation.[3] However, individuals with PSC do not benefit from immunosuppressive treatments, and about 25% of patients develop recurrent disease after liver transplantation under immunosuppressive treatment.[4] Currently, there is no effective treatment to prevent PSC disease progression, emphasising the need to understand the molecular mechanisms of

PSC pathogenesis in order to develop new therapeutic strategies. Genetic risk associations within the human leucocyte antigen (HLA) region, as well as non-HLA risk genes have been described.[5–7] Within the HLA-region, several HLA-DR/DQ risk haplotypes have been identified,[8] while limited data are available regarding HLA-DP associations in PSC.[9] The high linkage disequilibrium between HLA-class II alleles requires functional validation of potential risk alleles.

Intrahepatic immune cells, including natural killer (NK) cells, have been identified as sources of proinflammatory cytokines, including IFN-γ, driving persistent inflammation in PSC.[10] NK cells belong to the group of innate lymphoid cells (ILCs) and are highly enriched within the liver,[11] representing the largest subpopulation of intrahepatic ILCs.[12] NK cell functions—such as antiviral and antitumor activity and modulation of T cells[13 14]—are tightly regulated by integration of signals from multiple activating and inhibitory receptors, including natural cytotoxicity receptors (NCR). The NCR NKp44 binds to membrane-bound and soluble ligands,[15–17] including a subset of HLA-DP molecules,[18] providing a mechanism for interactions between NK cells and HLA-class II molecules. HLA-class II molecules are classically expressed on professional antigen-presenting cells, but epithelial cells can also express HLA-class II molecules after exposure to IFN-γ, inducing expression of the class II transcription activator.[19–22]

Here, we identified an HLA-DP PSC susceptibility haplotype *HLA-DPA1*02:01~DPB1*01:01* (OR 1.99, $p=6.69\times10^{-50}$) and demonstrate that NKp44 can bind to HLA-DPA1*02:01-DPB1*01:01, resulting in NKp44+NK cell activation. Human cholangiocyte organoids expressing the PSC risk molecule HLA-DPA1*02:01-DPB1*01:01 upregulated HLA-DP on stimulation with IFN-γ and showed an increased binding of NKp44, while degranulation of primary NKp44+NK cells was reduced against HLA-DPB1 KO compared with HLA-DP expressing WT cholangiocyte organoids. These findings identify a novel PSC risk haplotype *HLA-DP A1*02:01~DPB1*01:01* and provide clinical and functional data implicating NKp44+NK cells that recognise HLA-DPA1*02:01-DPB1*01:01 expressed on cholangiocytes in PSC pathogenesis.

MATERIALS AND METHODS

Liver and peripheral blood samples

Liver tissue and matched peripheral blood (PB) samples were obtained from individuals with PSC, primary biliary cholangitis (PBC) or autoimmune hepatitis (AIH) undergoing liver transplantation (ethics number PV4081) and individuals undergoing surgery for liver metastases (non-diseased resection margins; ethics number PV4898). Fresh biopsy samples were obtained from individuals undergoing mini-laparoscopic liver biopsy who consented for an additional biopsy to be taken for research purposes (PV5184). Clinical parameters are provided in online supplemental tables 1 and 2.

Immunohistochemical analyses of liver sections

Immunohistochemical analyses of PSC, PBC and AIH explant liver and non-autoimmune liver disease (AILD) control (non-alcoholic fatty liver disease, NAFLD) liver tissues were performed (ethics number PV4081). Clinical parameters are provided in online supplemental table 3. 5 µm sections of paraffin-embedded tissues were prepared. Tissues were deparaffinised followed by heat antigen retrival at 121°C for 10 min using S1699, pH6 (DAKO). Tissue sections were incubated with anti-HLA-DPA1 (Atlas, HPA017967) or isotype control rabbit poly IgG (abcam, ab37415) over night at 4°C. After washing with TBS-T, secondary staining was performed with goat α-rabbit-Biotin (LS-Bio, LS-C350860) for 30 min at room temperature. For detection, after washing of the slides, ABC-AP (VECTASTAIN, AK-5000) was added for 30 min, followed by Permanent Red staining (Zytomed Systems, ZUC001-125) for 7.5 min at RT. Subsequently, haematoxylin staining was performed. Image acquisition was performed using a Nikon eclipse Ni.

Immunofluorescence staining of liver biopsies

Immunofluorescence analyses were performed on residual histopathological material from liver biopsies of patients included in the livernet biobank (PV4081). Clinical parameters are provided in online supplemental table 4. Samples were dewaxed in xylene and rehydrated using a series of descending ethanol concentrations. Heat induced antigen retrieval was performed in Target retrieval solution pH9 (DAKO, S2367) using a pressure cooker in the microwave (20 min at 800W, 20 min at 600W). Samples were blocked with 5%BSA/PBS+0.25% Tween-20. Sections were incubated with primary antibodies over night at 4°C (CD56, Leica CD56-504-L-CE; CD45, Cell signalling 13917). Secondary staining was performed with goat-anti-mouse AF555 (Invitrogen, A327027) and donkey-anti-rabbit AF477 (Invitrogen, A21206) with incubation at room temperature for 1 hour, followed by nuclear staining with Hoechst 34580 (Sigma, 63493) for 30 min. Sections were mounted in Fluoromount-G (Invitrogen, 00-4958-02). Images were acquired with the same settings using a Nikon eclipse Ti microscope. Per sample, 3 fields-of-view at 200-fold magnification were examined for the presence of CD45+and CD45+CD56+ lymphocytes.

Isolation and staining of PBMCs

PB (EDTA-treated) was obtained from healthy donors on written informed consent (PV4780). PBMCs were isolated through density-gradient centrifugation and surface molecule expression was analysed by flow cytometry using antibodies described in online supplemental table 5. Samples were washed, fixed in 4% paraformaldehyde/phosphate buffered saline (PFA/PBS) and analysed using a BD LSRFortessa.

Mechanic dissociation of liver tissue and staining of intrahepatic lymphocytes

Intrahepatic lymphocytes were isolated as previously described.[23] Surface molecules expressed by intrahepatic lymphocytes were stained using the following antibodies: anti-CD45-AF700, anti-CD56-BUV395, anti-CD16-BV785, anti-CD3/CD14/CD19-BV510, anti-NKp44-PE, anti-NKp46-BV711, anti-CXCR6-BV421, anti-CD69-PerCP-Cy5.5 and LIVE/DEAD Fixable Near-IR Dead Cell Stain. Cells were fixed in 4% PFA/PBS. For intracellular staining, cells were fixed and permeabilised using FoxP3 Transcription Factor staining buffer set (Invitrogen) and subsequently stained with RORγt PE-CF594. Samples were analysed using a BD LSRFortessa.

Processing of fresh liver biopsies for flow cytometric analysis of intrahepatic lymphocytes

Biopsy samples were rinsed in cold wash medium (Iscove's Modified Dulbecco's Medium (IMDM)/2% FBS/1% penicillin/streptomycin) and digested in IMDM supplemented with 2.5 mg/mL collagenase and 0.1 mg/mL DNAseI for 30 min at 37°C in a water bath. Digestion was stopped by adding cold wash medium and samples were passed through a 70 µm cell strainer. After washing

in wash medium and subsequently in PBS, surface staining was performed as described above.

Stimulation of intrahepatic lymphocytes

Cryopreserved intrahepatic lymphocytes were thawed. Lymphocytes were stimulated in the presence of brefeldin A (5 µg/mL) with PMA (phorbol 12-myristate 13-acetate, 50 ng/mL) and ionomycin (1 µg/mL) in RPMI/10% FBS for 5 hours (37°C, 5% CO_2) or left unstimulated under equal conditions. Anti-CD16-FITC and anti-NKp44-PE were added when starting the stimulation. After 5 hours, cells were washed and surface staining was performed using anti-CD3/CD14/CD19-AF700, anti-CD127-APC, anti-CD56-BV510, anti-CD45-PE-Cy5 and LIVE/DEAD Fixable Near-IR Dead Cell Stain. Cells were fixed and permabilised using FoxP3 Transcription Factor staining buffer set (Invitrogen). Subsequently, intracellular cytokine staining was performed using anti-TNF-BV605 and anti-IFNγ-PE/Cy7. Samples were analysed using a BD LSRFortessa.

HLA-DPA1 and HLA-DPB1 imputation and association analysis

PSC case and control cohorts of individuals of European ancestry from 14 countries in Europe and North America genotyped with Illumina's Immunochip have been previously described.[24] 6275 SNPs with minor allele frequencies>0.1% were extracted from the extended HLA region (chromosome 6, 25–34 Mb) and submitted to SNP Phasing (using SHAPEIT2[25]) and HLA allele imputation (using Beagle V.4.1[26] to fill missing SNP genotypes for typed markers, followed by HLA allele imputation with HIBAG[27]) at loci HLA-DPA1 and HLA-DPB1 at full context four-digit level.[28] HLA-DPA1 and HLA-DPB1 imputation was performed for a total number of 37 621 individuals (3,408 PSC cases and 34 213 controls). For the HLA-DPA1 locus imputation was not possible for 1 of 37 621 individuals. For the HLA-DPB1 locus imputation was not possible for 72 of 37 621 individuals. Logistic regression association analyses for individual HLA-DP alleles and DPA1-DBP1 haplotype combinations was performed, adjusted for the first seven principal components from principal component analysis using FlashPCA2.[29]

Recombinant human NKp44/Fc-construct binding on HLA-Class II single-antigen beads

Binding of NKp44 to specific HLA-DP molecules was assessed using LABScreen Single Antigen HLA Cclass II—Group 1 kit, as previously described.[18] Details are provided in online supplemental information.

Isolation of NK cells, NK cell stimulation and degranulation assay

NK cells were enriched from PBMC via negative selection using EasySep Human NK Cell Enrichment Kit (Stemcell). NK cells were stimulated in RPMI-1640 (Gibco)/10% FBS (Capricorn)+250 U/mL IL2 (Peprotech)+10 ng/mL IL15 (Peprotech) for 5–7 days at a concentration of 1×10^6 cells/mL at 37°C/5% CO_2. NK cell degranulation was assessed in a plate-bound assay, as previously described.[18] Details are provided in online supplemental information.

Generation of cholangiocyte organoids

Cholangiocyte organoids were generated from human liver tissue as previously described.[30] In brief, liver tissue was cut in small pieces and washed twice in wash medium (Dulbecco's Modified Eagle Medium (DMEM) high glucose, GlutaMAX, pyruvate with 1% FBS and 1% Pencillin/Streptomycin). Single cells were obtained on enzymatic digestion, using EBSS containing 2.5 mg/mL collagenase D and 0.1 mg/mL DNase 1 at 37°C. Digestion was stopped by adding 4°C cold wash medium. Cell suspensions were passed through a 70 µm cell strainer. Cells were washed twice and resuspended in Advanced DMEM/F-12 containing 1% GlutaMAX, 10 mM HEPES and 1% Penicillin/Streptomycin (AD+++). Cholangiocytes were collected by centrifugation and seeded in droplets of isolation medium (hL-ISO, online supplemental table 6) and BME-2 at a ratio of 1:4. Hl-ISO was added and cells were cultured at 37°C/5% CO_2. Medium was exchanged every 2–3 days. After the first 5 days of culture, medium was changed to expansion medium (hL-EM, online supplemental table 6). Cholangiocyte organoids were passaged every 7–10 days.

Generation of HLA-DPB1 KO cholangiocyte organoids

CRISPR/Cas9 mediated knockout of HLA-DPB1 was performed targeting HLA-DPB exon 1 (spacer sequence GGAAACCT-GCAGAACCATCA) and is described in more detail in online supplemental information.

Immunofluorescence staining of organoids

Immunofluorescence staining of organoids was performed as previously described.[31] Details are provided in online supplemental information.

Flow cytometric analysis of cholangioyte organoids

Three-dimensional (3D)-matrix droplets containing organoids were disrupted and washed twice in AD+++. Organoids were dissociated to single cells by digestion in TrypLE Express Enzyme (Gibco) at 37°C for up to 40 min. Digestion was stopped by adding cold AD+++. Cells were washed, taken up in PBS and transferred to a V-bottom 96 well-plate. Cells were subsequently stained for 20 min at RT in the dark, washed, fixed in 4% PFA/PBS and analysed using a BD LSRFortessa.

NKp44/Fc-construct staining of cholangiocyte organoids

Organoids were dissociated to generate single cells as described above, washed and stained with NKp44/Fc-chimaera (R&D Systems) at a final concentration of 25 µg/mL for 15 min at 4°C. Secondary staining was performed with F(ab)2-goat-anti-human-Fc R-PE antibody (Invitrogen) for 15 min at 4°C. Cells were washed twice and stained with HLA-DP-APC (Leinco-Technologies) for 15 min at RT. Cells were fixed with 4% PFA/PBS and analysed at a BD LSRFortessa.

NK cell degranulation assay against cholangiocyte organoids

NK cells were isolated from cryopreserved PBMCs of autologous donors or individuals matched for HLA-Bw4/Bw6 and C1/C2 motifs to organoid donor, and stimulated as described above. WT and HLA-DPB1 KO organoids were expanded, stimulated with IFN-γ (200 U/mL, 72 hours) and dissociated to single cells. Prestimulated NK cells were resuspended in RPMI-1640/10% FBS at final concentration of 2×10^5 cells/mL. Cholangiocyte organoids and NK cells were distributed to the respective conditions at a E:T ratio of 1:10 and anti-CD107a-BV785 (BioLegend) was added. Plate-bound anti-NKp44 and PBS only served as positive and negative controls. Cells were incubated for 5 hours at 37°C/5% CO_2, and subsequently stained with anti-CD3-BV510,

anti-CD56-BV605, anti-CD16-FITC, anti-NKp44-AF647, anti-CD69-BV421 (all BioLegend) and LIVE/DEAD Fixable Near-IR Dead Cell Stain (Invitrogen). Cells were washed, fixed in 4% PFA and analysed at a BD LSRFortessa.

Data analysis and statistics

Flow cytometry data were analysed using FlowJo V.10 (Tree-Star). Statistical analyses were performed using GraphPad Prism V.9. Statistic tests used are indicated in the respective sections.

Patient and public involvement

Patients or public were not involved in the design or conduction of our research.

RESULTS

Increased expression of HLA-DP on intrahepatic bile ducts and decreased frequency of intrahepatic NKp44+ NK cells in PSC

Intrahepatic and extrahepatic bile ducts are the site of manifestation of PSC, where inflammation leads to scaring of the bile ducts. PSC is associated with increased levels of IFN-γ[10 32] that induces HLA-class II expression on non-haematopoietic cells.[19] As HLA-DP is a cellular ligand for the activating NK cell receptor NKp44, we aimed to assess whether intrahepatic HLA-DP expression can influence NK cell activation and therefore performed immunohistochemical analyses of HLA-DP on liver sections from explant livers of individuals with PSC, PBC and AIH, and liver tissue from individuals with NAFLD serving as non-AILD control. As expected, explant livers of individuals with end-stage liver disease showed bile duct proliferation, resulting in larger areas of intrahepatic bile ducts compared with NAFLD. While weak expression of HLA-DP was detectable on the biliary epithelium of donors with NAFLD, AIH and PBC, it was much more prominent on the biliary epithelium of individuals with PSC (figure 1A, online supplemental figure 1A, B).

Next, liver samples and matched PB samples of individuals with PSC, PBC, AIH and control samples from non-diseased resection margins of liver metastases as well as fresh liver biopsy specimen of individuals with PSC, AIH, PBC or non-AILD controls were used to determine the expression of NKp44 on NK cells. Frequencies of NKp44+NK cells were significantly higher in non-diseased control liver tissues compared with matched PB samples (figure 1B). NK cells constituted a large population of intrahepatic (ih) lymphocytes (figure 1C, online supplemental figure 2A), as previously described.[11] While frequencies of ihNK cells were comparable in PSC, PBC and non-AILD, individuals with AIH showed significantly decreased frequencies compared with individuals with PSC (figure 1C). To further characterise NK cell frequencies in liver tissues, we performed immunofluorescence analyses of CD45 and CD56 expression on liver biopsies of individuals with PSC, AIH, PBC and NAFLD without liver cirrhosis. While AIH biopsies showed a dominant infiltration of CD45+lymphocytes, we did not detect significant differences in absolute numbers of CD56+CD45+ cells quantified per field of view between PSC, PBC, AIH and NAFLD samples (online supplemental figures S3, 4). In line with previously published data, CD56 expression was also detectable on bile ducts of PSC, PBC and AIH biopsies[33].

To further characterise liver-derived NK cell populations by flow cytometry, liver residency of NK cells was defined by expression of CXCR6.[34] Frequencies of liver-resident (lr) NK cells did not differ between individuals with PSC and other AILD or non-AILD controls (figure 1D, online supplemental figure 2A). However, individuals with PSC, but not individuals with other AILD or non-AILD controls, showed significantly reduced frequencies of NKp44+ihNK and lrNK cells (figure 1E). Furthermore, no correlation between grade of fibrosis and frequencies of NK cells within intrahepatic lymphocytes or expression of NKp44 was detectable (online supplemental figure 5). As ILCs can also express NKp44, we employed a combined staining of CD127 and RORγt with NKp44, and showed that the detected NKp44+NK cell populations belong to the group of conventional intrahepatic and liver resident NK cells, while NKp44+CD127+ RORγt+ILCs were very rare (range: 0.0%–1.58% of CD3−/CD14−/CD19− intrahepatic lymphocytes; online supplemental figure 6). In contrast to the reduced frequencies of NKp44 expression on intrahepatic or liver-resident NK cells in PSC, no alterations of NKp44 expression was detectable on PB NK cells (online supplemental figure S2D).

We next evaluated potential differences in the activation status of NK cells in PB or liver samples. No significant differences in expression of the activating NCR NKp46 on intrahepatic or PB NK cells of people with PSC compared with control individuals was observed. Expression of CD69, a marker of liver residency and NK cell activation,[34 35] was comparable on intrahepatic NK cells of all groups, while individuals with PBC or AIH showed significantly higher frequencies of CD69+PB NK cells compared with non-AILD controls (online supplemental figure 2B–F). We further investigated the functional capacities of NKp44+ihNK cells on stimulation. NKp44−ihNK cells and NKp44+ihNK cells of PSC, other AILD and non-diseased resection margins of liver metastases exhibited similar expression of IFN-γ and TNF after stimulation with PMA/ionomycin (online supplemental figure 7). Taken together, individuals with PSC exhibited elevated expression of HLA-DP on intrahepatic bile ducts and reduced frequencies of NKp44+ihNK cells.

Identification of HLA-DP A1*02:01 B1*01:01 as a susceptibility haplotype for PSC

Several GWAS studies have identified risk genes for PSC, but the impact of HLA-DP allotypes on PSC has not yet been investigated. Since we detected an elevated expression of HLA-DP on intrahepatic bile ducts in individuals with PSC, we investigated associations between specific HLA-DP alleles and the risk to develop PSC. *HLA-DPA1* and *HLA-DPB1* imputation and association analyses in 3,408 PSC cases and 34 213 controls of European ancestry were performed and newly identified two PSC risk alleles (*HLA-DPA1*02:01* and *DPB1*01:01*) and two protective alleles (*HLA-DP A1*01:03* and *DPB1*03:01*) with genome-wide statistical significance ($p<5\times10^{-8}$) (table 1, online supplemental table 7). As these analyses identified one HLA-DPA and one HLA-DPB allele associated with risk or protection from PSC, respectively, and that haplotypes consisting of the respective HLA-DPA and DPB alleles have been described,[36] we performed HLA-DP haplotype analyses. The HLA-DP haplotype analysis revealed that *HLA-DPA1*02:01~DPB1*01:01* was highly significantly associated with an increased risk of PSC (OR 1.99, $p=6.69\times10^{-50}$), whereas *HLA-DPA1*01:03~DPB1*03:01* was protective (OR 0.78, $p=3.18\times10^{-9}$) (table 1, online supplemental table 8). Taken together, these analyses of 3408 PSC cases and 34 213 controls identified *HLA-DPA1*02:01~DPB1*01:01*, with a haplotype frequency of 9.5% in PSC cases and 4.7% in controls, as a highly significant susceptibility haplotype for PSC.

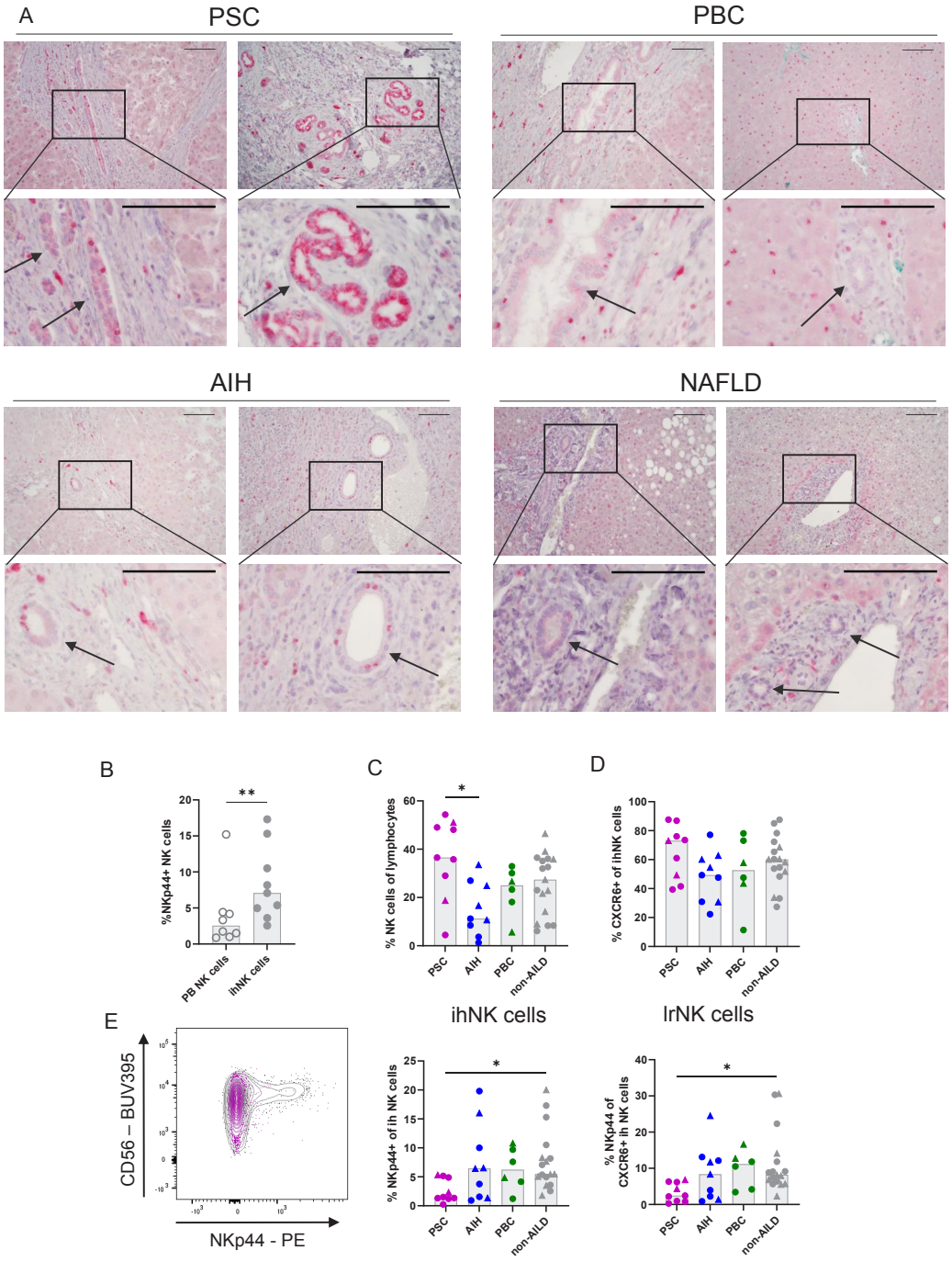

Figure 1 Upregulation of HLA-DP expression and reduced frequencies of intrahepatic NKp44+NK cells in individuals with PSC. (A) Representative images of immunohistochemical analyses of HLA-DP (permanent red) in PSC, PBC and AIH-affected liver sections and non-AILD controls (NAFLD). Scale bars indicate 100 µm. Arrows point at intrahepatic bile ducts. (NAFLD n=6; PSC n=8, AIH n=6, PBC n=7). (B) Frequencies of NKp44+NK cells in matched peripheral blood (PB) and intrahepatic (ih) NK cells of non-AILD liver tissue. (C) Frequencies of NK cells within intrahepatic (ih) lymphocytes of individuals with PSC, AIH, PBC and non-AILD controls. (D) Frequencies of CXCR6+NK cells within ihNK cells of individuals with PSC, AIH, PBC and non-AILD controls. (E) Expression of NKp44 by intrahepatic (ih; middle panel), liver-resident (lr; right panel) NK cells of individuals with PSC, AIH, PBC and non-AILD controls. Left panel: representative flow cytometry plot (non-AILD—grey, PSC—magenta). Dots represent explant liver samples and resection margins of liver metastases. Triangles represent fresh liver biopsies. Bars indicate the median. Wilcoxon test was used to assess statistical differences between matched PB and liver samples (B). **p=0.0078. Kruskal-Wallis test (Dunn's post-test) was used to assess statistical differences between PSC and control groups (C–E). (C) *p=0.0190, (E) ih NK cells *p=0.0169; lr NK cells *p=0.0120. AIH, autoimmune hepatitis; AILD, autoimmune liver disease; NAFLD, non-alcoholic fatty liver disease; PBC, primary biliary cholangitis; PSC, primary sclerosing cholangitis.

Table 1 Four HLA-DPA1 and HLA-DPB1 alleles are associated with PSC in Europeans (3408 cases and 34 213 controls) at genome-wide significance level ($p<5\times10^{-8}$)

HLA allele/haplotype	AF (cases)	AF (controls)	P value	OR (95% CI)
DPA1*01:03	0.80	0.83	8.91×10^{-11}	0.81 (0.76 to 0.86)
DPA1*02:01	0.17	0.14	7.49×10^{-16}	1.32 (1.23 to 1.41)
DPB1*01:01	0.10	0.05	6.11×10^{-42}	1.83 (1.68 to 2.00)
DPB1*03:01	0.10	0.13	2.82×10^{-9}	0.78 (0.72 to 0.85)
DPA1*02:01|DPB1*01:01	0.095	0.047	6.69×10^{-50}	1.99 (1.82 to 2.18)
DPA1*01:03|DPB1*03:01	0.103	0.126	3.18×10^{-9}	0.78 (0.72 to 0.85)

Haplotype analysis using these four genome-wide significant HLA alleles revealed two haplotypes at genome-wide significance level.
AF of HLA allele estimated from Immunochip data of PSC cases and controls.
P/OR: P value and corresponding allelic OR and 95% CI regarding the presence of the HLA allele. Full association results for each alleles and haplotypes tested are shown in online supplemental table 7 and 8.
AF, allele frequency; PSC, primary sclerosing cholangitis.

HLA-DPA1*02:01-DPB1*01:01 molecules bind to NKp44 and are associated with high HLA-DP surface expression

Although most studies have focused on HLA-class II interactions with T cells, we recently described that a subset of HLA-DP molecules can bind the activating NK cell receptor NKp44.[18] Given the elevated expression of HLA-DP on intrahepatic bile ducts of individuals with PSC and the reduced frequencies of ihNKp44+NK cells, we investigated whether the HLA-DP molecules associated with differential PSC risk exhibited differences in binding to NKp44. Beads coated with specific HLA-DP molecules were co-incubated with an NKp44/Fc-construct and binding was quantified using a secondary antibody against Fc. We confirmed that HLA-DPA1*02:01-DPB1*01:01 binds to NKp44, while HLA-DPA1*01:03-DPB1*03:01 did not bind to NKp44 (figure 2A).[18] Assessment of NKp44-binding to a total of 31 HLA-DP molecules showed that six other HLA-DP molecules bound to NKp44 in addition to HLA-DPA1*02:01-B1*01:01 (figure 2A). Of these six other NKp44-binding haplotypes, only the *HLA-DPA1*01:03~DPB1*04:01* allele combination was present in the cohorts included in the analysis with a high frequency of 44%, whereas the other five binding HLA-DP molecules were very rare (frequencies of 1% or below). *HLA-DPB1*04:01* was, however, not associated with an elevated risk for PSC (online supplemental table 7).

HLA-DPB1 alleles can be divided into two groups based on SNP rs9277534A/G, which determines the expression level of the HLA-DP beta-chain.[37] While *HLA-DPB1*04:01*—the most common beta chain that forms an NKp44-binding HLA-DP molecule with the *HLA-DPA1*01:03* allele—is linked to rs9277534A (low expression), the PSC risk allele *HLA-DPB1*01:01* is linked to rs9277534G (high expression) (figure 2A). To confirm that the NKp44-binding HLA-DPA1*02:01~DPB1*01:01 PSC risk haplotype was indeed expressed at high levels, flow cytometric analysis of HLA-DP protein expression on the surface of B cells, which constitutively express HLA-DP, from healthy donors was performed. As previously described,[38] individuals with HLA-DP haplotypes linked to rs9277534G/G had high HLA-DP expression levels (MdFI of HLA-DP=3469), whereas HLA-DP haplotypes linked to rs9277534A/A exhibited low surface expression of HLA-DP (MdFI of HLA-DP=1877, p=0.034, figure 2B). Within our cohort, we had access to PBMCs from individuals that were heterozygous for the PSC risk haplotype *HLA-DPA1*02:01~DPB1*01:01* (rs9277534G) and encoded for a second HLA-DPB1 allele linked to rs9277534A (low expression). In these individuals, HLA-DP expression was comparable to that observed in the rs9277534G/G individuals (MdFI of HLA-DP=2984) (figure 2B, online supplemental table 9). Taken together, these data identify the PSC risk haplotype *HLA-DPA1*02:01~DPB1*01:01* as an HLA-DP molecule that is both highly expressed and binds to NKp44, while other common HLA-DP molecules not associated with PSC risk were either not binding NKp44 or expressed at low surface levels. Therefore, we hypothesised that the combination of high expression and NKp44-binding of HLA-DPA1*02:01-DPB1*01:01 molecules might result in the activation of NKp44+NK cells in the liver, contributing to the risk of developing PSC.

Binding of HLA-DPA1*02:01~DPB1*01:01 molecules to NKp44 leads to activation of NK cells

After confirming that NKp44 binds to HLA-DPA1*02:01-DPB1*01:01 molecules in a non-cellular assay, we assessed whether this interaction also activated NKp44+NK cells, using a plate-bound degranulation assay with primary NK cells. Prior to the degranulation assay, NK cells were stimulated with IL-2 and IL-15 to induce expression of NKp44. Incubation of NKp44-expressing NK cells on plate-bound HLA-DPA1*02:01-DPB1*01:01 molecules led to a significantly increased degranulation of NK cells compared with plate-bound HLA-DPA1*01:03-DPB1*03:01 molecules (percentages CD107a+NK cells minus negative control: median 3.24 IQR 1.91–8.02 vs median 1.03 IQR 0.31–3.22, p=0.0078) (figure 3A). Blocking of NKp44 prior to incubation with plate-bound anti-NKp44 or HLA-DPA1*02:01-DPB1*01:01 significantly reduced expression of CD107a by NK cells (figure 3B). Next, we investigated the effect of NKp44-binding to HLA-DP on NKp44 expression levels of NK cells, as binding of activating NK cell receptors to their respective ligands has been described to subsequently induce internalisation of the receptor.[39] Expression levels of NKp44 were reduced on binding to plate-bound HLA-DPA1*02:01-DPB1*01:01, while plate-bound HLA-DPA1*01:03-DPB1*03:01 molecules had no effect on expression levels of NKp44 (figure 3C). Taken together, these data show that binding of HLA-DPA1*02:01-DPB1*01:01 molecules to NKp44 leads to activation of primary human NKp44+NK cells and subsequently reduced surface expression of NKp44. These data furthermore provide a correlate for the decreased expression of NKp44 observed on intrahepatic NK cells of individuals with PSC (figure 1E), as HLA-DP expression was upregulated on intrahepatic bile ducts in individuals with PSC (figure 1A).

Increased binding of NKp44 to HLA-DP-expressing cholangiocytes and HLA-DP-dependent activation of NKp44+ NK cells

The above results led to the hypothesis that elevated expression of HLA-DP on bile ducts of individuals with PSC mediates activation of ihNK cells via NKp44. To test this hypothesis, we generated cholangiocyte organoids from human liver tissues. Cholangiocyte organoids grew in cystic structures and expressed cholangiocyte markers such as Cytokeratin 19 (figure 4A,B). On stimulation with IFN-γ, cholangiocyte organoids strongly upregulated HLA-DP protein expression (figure 4C and D). Using cholangiocyte organoids from four individuals with the PSC risk haplotype *HLA-DPA1*02:01~DPB1*01:01*, we assessed the consequence of HLA-DP upregulation on NKp44 binding, using NKp44/Fc-fusion constructs. Binding of NKp44/Fc-construct to IFN-γ-stimulated HLA-DP+cholangiocytes was significantly

A

Number	α chain	β chain	rs9277534
-	negative control		
+	positive control		
1	A1*01:03	B1*01:01	G
2	A1*02:01	B1*01:01	G
3	A1*01:03	B1*02:01	A
4	A1*02:02	B1*05:01	G
5	A1*01:03	B1*03:01	G
6	A1*01:05	B1*03:01	G
7	A1*02:01	B1*03:01	G
8	A1*01:03	B1*04:01	A
9	A1*01:03	B1*04:02	A
10	A1*02:01	B1*05:01	G
11	A1*02:01	B1*06:01	G
12	A1*01:03	B1*06:01	G
13	A1*02:01	B1*09:01	G
14	A1*02:02	B1*10:01	G
15	A1*01:03	B1*11:01	G
16	A1*01:03	B1*28:01	n.d.
17	A1*02:01	B1*13:01	G
18	A1*02:02	B1*13:01	G
19	A1*03:01	B1*13:01	G
20	A1*02:01	B1*14:01	G
21	A1*02:01	B1*15:01	G
22	A1*02:01	B1*17:01	A
23	A1*02:01	B1*18:01	G
24	A1*01:05	B1*18:01	G
25	A1*01:04	B1*18:01	G
26	A1*01:03	B1*19:01	G
27	A1*03:01	B1*20:01	G
28	A1*01:03	B1*23:01	A
29	A1*01:05	B1*28:01	n.d.
30	A1*04:01	B1*28:01	n.d.
31	A1*02:02	B1*11:01	G

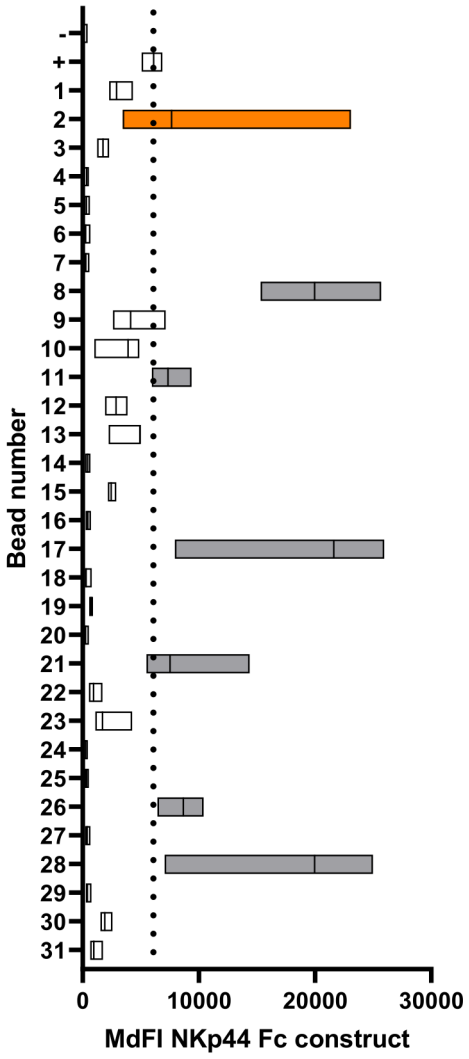

B

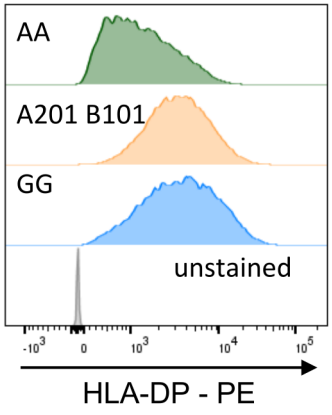

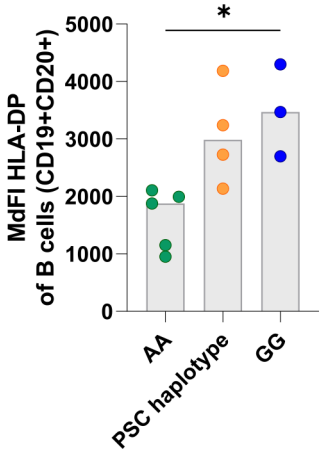

Figure 2 PSC HLA-DP susceptibility alleles encode for an NKp44-binding HLA-DP molecule (A) Median fluorescence intensity (MdFI) of NKp44 Fc-construct binding (x-axis) to HLA-DP coated beads. Depicted are median (line) and range (boxes) of three individual experiments. The dotted line represents the MdFI of the positive control. Orange: HLA-DPA1*02:01-DPB1*01:01 (consisting of both PSC risk alleles), grey: all other HLA-DP molecules with NKp44/Fc-construct binding above the positive control. Left: Table indicating HLA-DP alleles of the coated beads. Association of the HLA-DP beta-chain alleles with the SNP rs9277534 is marked according to Schöne *et al*.[37] (B) MdFI of HLA-DP expression on CD3- CD19+CD20+ B cells of healthy donors encoding for HLA-DP haplotypes linked to rs9277534G/G, rs9277534A/A or *HLA-DPA1*02:01~DPB1*01:01* rs9277534G/A. Each dot represents results from one donor. Bars indicate the median. Kruskal-Wallis test with Dunn's post-test was used to assess statistical differences between the groups. *p=0.034. PSC, primary sclerosing cholangitis.

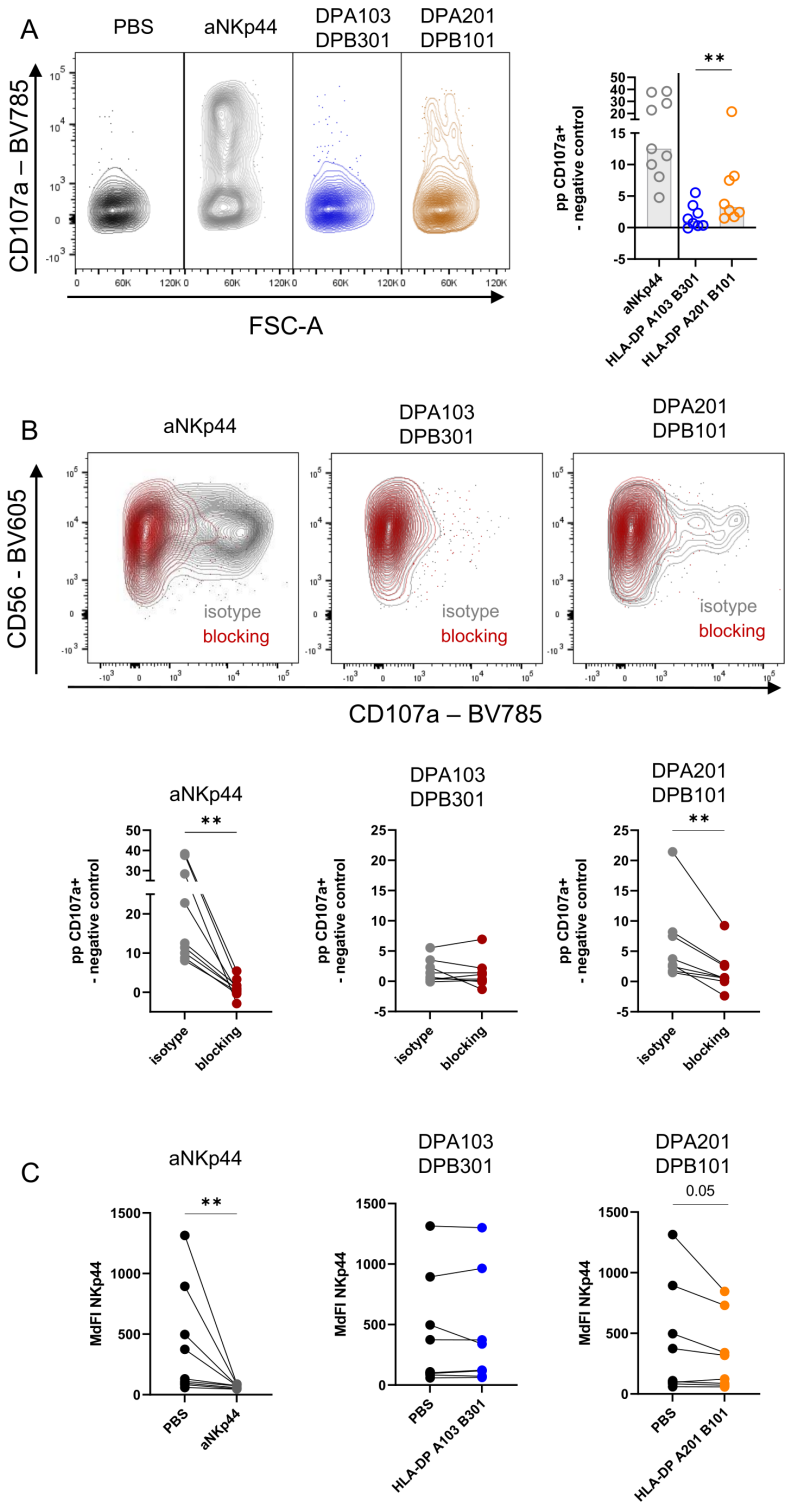

Figure 3 PSC susceptibility haplotype *HLA-DP A1*02:01~DPB1*01:01* enables binding to NKp44, leading to activation of NK cells (A) Left panel: representative plots of CD107a expression (y-Axis) of prestimulated NK cells on incubation with plate-bound anti-NKp44 (grey), HLA-DPA1*01:03-DPB1*03:01 (blue), HLA-DPA1*02:01-DPB1*01:01 (orange) or PBS as negative control (black). Right panel: percentages of CD107a+NK cells in the plate-bound degranulation assay after incubation with the respective HLA-DP molecules minus PBS negative control. Wilcoxon-signed rank test was used to assess statistical differences between the different HLA-DP molecules; **p=0.0078. (B) Representative plots (upper panel) and percentages of CD107a+NK cells (lower panel) in a plate-bound degranulation assay after incubation with anti-NKp44 (left) or the respective HLA-DP molecules (middle HLA-DPA1*01:03-DPB1*03:01, right HLA-DPA1*02:01-DPB1*01:01) minus PBS negative controls after preincubation with anti-NKp44 blocking antibody or the isotype control antibodies. Wilcoxon-signed rank test was used to assess statistical differences between the groups. **p=0.0039 (aNKp44); **p=0.0078 (HLA-DPA201-DPB101). (C) MdFI of NKp44 expression on NK cells in the plate-bound degranulation assay on incubation with PBS and plate-bound anti-NKp44 (left), HLA-DPA1*01:03-DPB1*03:01 (middle), and HLA-DPA1*02:01-DPB1*01:01 (right). Lines connect the corresponding conditions of one donor. Wilcoxon-signed rank test was used to assess statistical differences between the groups. **p=0.0039 (aNKp44); p=0.0547 (HLA-DPA201-DPB101).

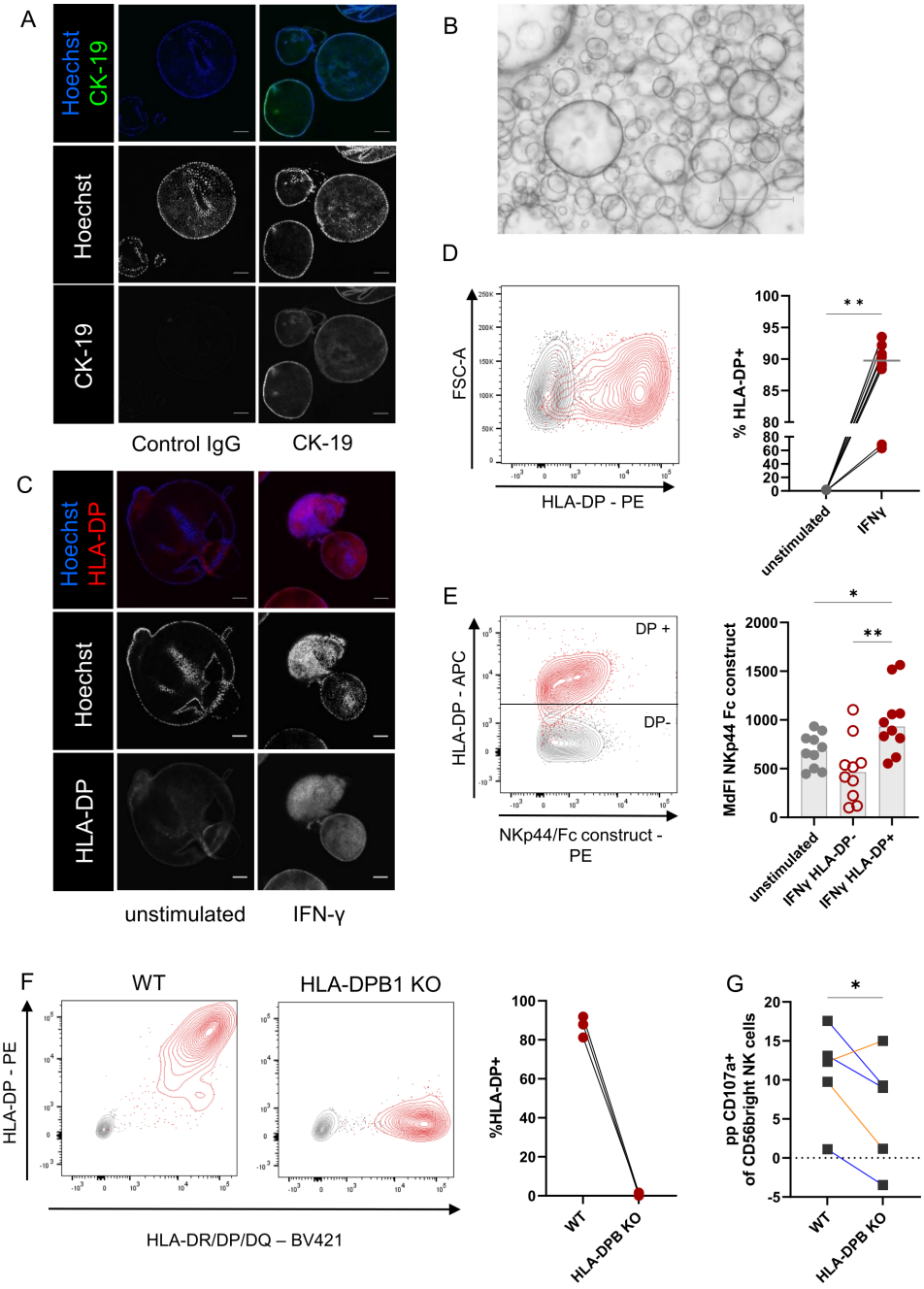

Figure 4 Increased binding of NKp44/Fc construct to HLA-DP expressing cholangiocyte organoids and reduced degranulation of NK cells towards HLA-DPB1 KO cholangiocyte organoids (A) Immunofluorescence analyses of cholangiocyte organoids for Cytokeratin 19 (CK-19—green) and Hoechst blue (blue). Full staining (right panel) and control IgG (left panel). Scale bar represents 100 µm. (B) Light microscopy images of cholangiocyte organoids showing cystic structures. Scale bar represents 750 µm. (C) Immunofluorescence analyses of cholangiocyte organoids for Hoechst (blue) and HLA-DP PE (red) unstimulated (left panel) and IFN-γ-stimulated (right panel). Scale bar represents 100 µm. (D) Left panel: Representative plot of HLA-DP expression (x-Axis) of unstimulated (grey) and IFNγ-stimulated cholangiocytes from organoids (red). Right panel: Percentage of HLA-DP+cholangiocytes from organoids within unstimulated or IFN-γ-stimulated cultures. n=10, from five donors in three individual experiments. Wilcoxon-signed rank test was used to assess statistical differences between the matched conditions. **p=0.002. (E) Left panel: representative plot of HLA-DP expression (y-Axis) and NKp44/Fc-construct binding (x-axis) of cholangiocytes from organoids unstimulated (grey) or IFN-γ-stimulated (red). Right panel: MdFI of NKp44/Fc-construct binding to cholangiocytes from organoids unstimulated (grey) or IFN-γ-stimulated HLA-DP- populations (red circles) and IFN-γ-stimulated HLA-DP+populations (red dots). Friedman test with Dunn's post-test was used to assess statistical differences between the groups. *p=0.0417; **p=0.001. (n=10, from four individual donors; performed in three individual experiments). (F) Expression of HLA-DP on WT and HLA-DPB1 KO cholangiocytes from organoids after IFN-γ-stimulation, performed in tree individual experiments. Left: representative plot: HLA-DP (y-axis) and HLA-DR/DQ/DP-expression (x-axis) of WT (left) or HLA-DPB1 KO (right) cholangiocytes from organoids after stimulation with IFN-γ (red) and unstimulated control (grey), right: graph showing frequencies of HLA-DP+cholangiocyte organoid cells. (G) Depicted is the CD107a expression of prestimulated NK cells after co-incubation with IFN-γ-stimulated WT or HLA-DPB1 KO organoids minus PBS negative control. (NK cell donors: autologous NK cells in triplicate—blue lines; HLA/KIR-ligand matched NK cells, one donor in duplicate—orange lines). One-tailed t-test to test the hypothesis that HLA-DPB KO leads to reduced degranulation of NKp44+NK cells, p=0.044.

increased compared with IFN-γ-stimulated HLA-DP- cholangiocytes or matched unstimulated controls (figure 4E, online supplemental table 10), demonstrating that IFN-γ-induced expression of HLA-DP on cholangiocytes can serve as a ligand for NKp44. To assess the functional impact of this receptor/ligand interaction on the surface of human cholangiocytes for NK cell activation, we generated HLA-DPB1 knock-out organoids using parental organoids encoding for the PSC risk haplotype *HLA-DPA1*02:01~DPB1*01:01*. After stimulation with IFN-γ, HLA-DPB1 KO organoids showed no surface expression of HLA-DP, while pan-HLA-class II expression was similar to parental WT organoids (figure 4F). Coincubation of autologous or HLA/KIR ligand-matched NKp44+NK cells with IFN-γ-stimulated HLA-DPB1 KO or WT organoids demonstrated reduced degranulation of NK cells against HLA-DPB1 KO organoids (figure 4G). Taken together, these results are consistent with HLA-DPA1*02:01-DPB1*01:01-dependent activation of NKp44+NK cells by human cholangiocytes, providing a functional correlate for the high OR for PSC risk associated with *HLA-DPA1*02:01~DPB1*01:01* in individuals encoding for this HLA-DP haplotype.

DISCUSSION

Despite PSC being an immune-mediated disease, classical immunosuppressive treatments show no benefit,[40] and there are no targeted therapies to treat PSC to date. In this study, we identified the HLA-DP PSC susceptibility haplotype *HLA-DPA1*02:01~DPB1*01:01* (OR 1.99, $p=6.69\times10^{-50}$) and demonstrate that NKp44 can bind to HLA-DPA1*02:01-DPB1*01:01, resulting in activation of NKp44+NK cells. Furthermore, cholangiocyte organoids generated from primary human cholangiocytes encoding for the PSC risk haplotype *HLA-DPA1*02:01~B1*01:01* showed upregulation of HLA-DP on stimulation with IFN-γ, and HLA-DP-dependent activation of primary NKp44+NK cells. This study identifies *HLA-DPA1*02:01~DPB1*01:01* as novel risk haplotype for PSC and implicates HLA-DP/NKp44-mediated NK cell activation in the pathogenesis of PSC.

Although the immunopathogenesis of PSC remains incompletely understood, studies have shown that IFN-γ levels in individuals with PSC are elevated,[10 32] which is a critical inducer of HLA-class II expression on non-haematopoietic cells, such as epithelial cells.[19 41] Multiple HLA-DR and –DQ risk haplotypes for PSC have been identified so far,[8] while data on HLA-DP association with PSC are scarce,[9] and functional data supporting the clinical relevance of the described HLA-class II associations are lacking. The HLA-class II region exhibits high linkage disequilibrium between the HLA-DR, HLA-DQ and HLA-DP loci, most prominent between the DR and DQ loci and less pronounced between DR-DQ and -DP.[42] HLA-DP associations with disease risk have been described for different immune-mediated and infectious diseases, including graft-versus-host disease, AIH and hepatitis B virus infection.[38 43–45] These disease associations have been linked to the SNP rs9277534 located in the 3' untranslated region of HLA-DPB that regulates the expression level of the HLA-DP beta-chain, and segregates HLA-DP alleles into HLA-DP molecules with low (rs9277534A) or high (rs9277534G) expression.[37 38 43] Interestingly, our analysis using 3,408 PSC cases and 34213 controls revealed no association for the SNP rs9277534 alone with PSC risk, but identified *HLA-DPA1*02:01~B1*01:01* as a highly significant risk haplotype for PSC (OR 1.99, $p=6.69\times10^{-50}$). The identified PSC risk haplotype *HLA-DPA1*02:01~DPB1*01:01* was present in 95/1000 affected individuals and 47/1000 non-affected controls. It may, therefore, be regarded as one of the genetic factors modulating the susceptibility for a multifactorial disease in individuals of European ancestry encoding for this HLA-DP haplotype. Importantly, both the risk haplotype *HLA-DPA1*02:01~DPB1*01:01* as well as the identified protective haplotype *HLA-DPA1*01:03~DPB1*03:01* (OR 0.78, $p=3.18\times10^{-9}$) are linked to rs9277534G.[37] This indicates that the association of HLA-DP haplotype and PSC risk is not mediated by HLA-DP expression levels alone, but required additional pathogenic mechanisms.

Studies of PSC pathogenesis have largely focused on adaptive immune responses towards gut-derived antigens and T-cell mediated inflammation.[46–49] Differential effects of NK cells in promoting or limiting hepatic damage have been described[50]; however, there is increasing evidence for a role of NK cells in driving inflammation in PSC.[10 51] Previous studies have shown that NK cells can be activated through the interaction of the NCR NKp44 with a subset of HLA-DP molecules, primarily including low-expressed HLA-DP molecules linked to rs9277534A, such as HLA-DPA1*01:03-DPB1*04:01.[18] The PSC risk haplotype *HLA-DPA1*02:01~DPB1*01:01* is a rare exception, representing a high-expressed HLA-DP molecules linked to rs9277534G that binds to NKp44. Our data furthermore demonstrate that HLA-DPA1*02:01-DPB1*01:01, but not other more common high-expressed HLA-DP molecules, such as HLA-DPA1*01:03-DPB1*03:01 identified here as a protective haplotype for PSC, activates primary NK cells in an NKp44-dependent manner. NKp44 was expressed more frequently on intrahepatic compared with PB NK cells, in accordance with published data,[52] but the frequencies of intrahepatic and liver-resident NKp44+NK cells were reduced in PSC-affected liver. These ex vivo data are consistent with the downregulation of NKp44 expression on NK cells after binding to HLA-DP we observed in vitro, indicating that reduced frequencies of intrahepatic NKp44+NK cells in PSC might result from NKp44 interactions with HLA-DP-expressing cells.

Studies of liver tissues from individuals with PSC have demonstrated that Kupffer cells and lymphoid cells, but also bile ducts, express HLA-class II molecules.[53] Human biliary epithelial cells have been shown to express lymphocyte adhesion molecules such as LCAM-1 and CD58[54] and to directly interact with lymphocytes, for example by presenting antigens to NKT cells.[55 56] However, there are no studies of NK cell/cholangiocyte interactions to date. Immunohistochemical analyses confirmed HLA-DP expression on intrahepatic bile ducts and showed elevated expression levels of HLA-DP in PSC livers compared with controls. To experimentally assess binding of NKp44 to HLA-DP on human cholangiocytes, we used cholangiocyte organoids. Cholangiocyte organoids as 3D-culture models have gained increasing importance over the last years in disease modelling and regenerative approaches.[30 57–59] Cholangiocyte organoids strongly upregulated HLA-DP molecules on stimulation with IFN-γ, and HLA-DP-positive cholangiocytes derived from individuals encoding for the PSC risk haplotype *HLA-DPA1*02:01~DPB1*01:01* showed increased binding of NKp44/Fc-constructs. Importantly, NKp44+NK cells exhibited higher degranulation in response to HLA-DPA1*02:01-DPB1*01:01-expressing cholangiocyte organoids than against cholangiocyte organoids in which HLA-DPB1 was knocked out. These data show that NKp44 can bind to cholangiocytes expressing the newly identified PSC risk HLA-DP molecule, resulting in HLA-DP-dependent activation of NKp44+NK cells. These findings implicate NK cells in PSC pathogenesis, emphasising the need of further studies to identify approaches to modulate NK cell activation in PSC, with the aim of attenuating disease progression.

The majority of individuals with PSC develops concomitant inflammatory bowel disease (PSC-IBD).[3] The protective and risk HLA-DP haplotypes discovered in this study were equally present in individuals with PSC-IBD and PSC without concomitant IBD (online supplemental table 11). HLA-DP expression on inflamed colonic epithelium may therefore also lead to activation of intestinal NKp44+NK cells and NKp44+RORγt+ILCs. The latter are known to develop independent of intestinal bacterial colonisation and produce IL-22 under homeostatic conditions,[60 61] while NKp44 engagement leads to the production of TNF,[62] and might therefore further promote intestinal inflammation in the context of elevated HLA-DP expression. As recently demonstrated in the context of ulcerative colitis, TNF production of intestinal NKp44+ILCs increased after incubation with NKp44-binding HLA-DP molecules compared with incubation with NKp44-non-binding HLA-DP molecules.[63] To determine the role of NKp44/HLA-DP interactions for colonic inflammation in PSC-IBD, further investigations are needed, including comparative analysis to ulcerative colitis and Crohn's disease. Taken together, these studies combining genetic association studies of PSC risk, patient samples and in vitro human cholangiocyte organoid models identify *HLA-DPA1*02:01~DPB1*01:01* as a highly significant risk haplotype for PSC that can be recognised by NKp44+NK cells and induce NK cell activation. These results implicate functional interactions between NKp44 and HLA-DP in progressive liver inflammation in PSC, providing a potential novel target for immunotherapies.

Author affiliations
[1]Ist Department of Medicine, University Medical Centre Hamburg-Eppendorf, Hamburg, Germany
[2]Leibniz Institute of Virology, Hamburg, Germany
[3]Institute of Clinical Molecular Biology, University of Kiel, Kiel, Germany
[4]Basic Science Program, Frederick National Laboratory for Cancer Research and Laboratory of Integrative Cancer Immunology, Center for Cancer Research, National Cancer Institute, Frederick, Maryland, USA
[5]Research Department Cell and Gene Therapy, Department of Stem Cell Transplantation, University Medical Center Hamburg-Eppendorf, Hamburg, Germany
[6]Institute of Anatomy and Experimental Morphology, University Medical Center Hamburg-Eppendorf, Hamburg, Germany
[7]International PSC Study Group, Hamburg, Germany
[8]Department of General & Abdominal Surgery, Asklepios Hospital Barmbek, Hamburg, Germany
[9]Institute of Pathology, University Medical Center Hamburg-Eppendorf, Hamburg, Germany
[10]Ragon Institute of MGH, MIT and Harvard, Cambridge, Massachusetts, USA
[11]III. Department of Medicine, University Medical Center Hamburg-Eppendorf, Hamburg, Germany
[12]Martin Zeitz Center for Rare Diseases and Hamburg Centre for Translational Immunology, University Medical Center Hamburg-Eppendorf, Hamburg, Germany
[13]Institute of Immunology, University Medical Center Hamburg-Eppendorf, Hamburg, Germany

Correction notice This article has been corrected since it published Online First. The author, Christoph Schramm, name has been corrected.

Acknowledgements The authors thank Ansgar Lohse for helpful discussions and critical input, Arne Düsedau and Jana Hennesen at the Core facility for Flow cytometry/FACS at the Leibniz Institute of Virology for assistance in cell sorting, and Roland Thünauer at the NIKON Centre of Excellence for assistance in image acquisition. We furthermore thank Christin Illig for technical assistance in organoid culture. The authors thank all clinicians and nurses who were involved in the acquisition of fresh liver biopsy samples.

Collaborators For the International PSC Study Group (IPSCSG): Hugh Harley, Dep Huynh, Peter Fickert, Michael Trauner, Emina Halilbasic, Johan Fevery, Werner Van Steenbergen, Isabelle Cleynen, Severine Vermeire, Schalk Van der Merwe, Henriette Ytting, Andrew Mason, Bertus Eksteen, Martti Farkkila, Chantal Housset, Olivier Chazouillères, Raoul Poupon, Christophe Corpechot, Tobias Weismüller, Verena Keitel, Dieter Häussinger, Christoph Schramm, Ansgar Lohse, Michael E Manns, Tim Lankisch, Daniel Gotthardt, Peter Sauer, Peter Schirmacher, Beate K. Straub, Vincent Zimmer, Andre Franke, Eva Ellinghaus, David Ellinghaus, Stefan Schreiber, Ruben Plentz, Hugh E. Mulcahy, Einar Björnsson, Oren Shibolet, Marco Marzioni, Pietro Invernizzi, Ana Lleo, Carlo Selmi, Luca Fabris, Annarosa Floreani, Atsushi Tanaka, Hiromasa Ohira, Yoshiyuki Ueno, Tom H Karlsen, Erik Schrumpf, Kirsten M Boberg, Lars Aabakken, Espen Melum, Johannes Hov, Trine Folseraas, Mette Vesterhaug, Piotr Milkiewicz, Ewa Wunsch, Andrzej Habior, Albert Pares, Alexander Knuth, Beat Müllhaupt, Andreas Geier, Joachim C. Mertens, Annika Bergquist, Sven Almer, Lina Lindstrøm, Niklas Björkström, Fredrik Rorsman, Maria Benito de Valle Villalba, Hanns-Ulrich Marschall, Peter L. Jansen, Ulrich Beuers, Cyriel Y. Ponsioen, Andreas E. Kremer, Serge Zweers, Rinse K Weersma, Frank G. Schaap, Henk R. van Buuren, David H. Adams, Gideon M Hirschfield, Evangelia Liaskou, Arthur Kaser, Graeme J. Alexander, George F. Mells, Richard N Sandford, Carl A Anderson, Jimmy Z Liu, Stephen Pereira, George Webster, Andrew Burroughs, Shahid A Khan, Simon D. Taylor-Robinson, David Jones, Alastair Burt, Simon M Rushbrook, Roger W Chapman, Kate Williamson, Emma L. Culver, Said Al Mammari, Keith Lindor, Christopher L Bowlus, David Shapiro, Mario Strazzabosco, Greg Everson, Steve Helmke, Cynthia Levy, Konstantinos N Lazaridis, Brian D Juran, Gregory Gores, Jayant Talwalkar, Nataliya Razumilava, David Goldberg, Dennis Black, Saul J. Karpen.

Contributors BFZ designed experiments, performed and analysed phenotypical and functional NK cell experiments, performed and analysed cholangiocyte organoid experiments, analysed immunohistochemistry experiments and performed and analysed immunofluorescence stainings of liver biopsies. DE performed and analysed the genetic studies. SS performed and analysed immunofluorescence stainings of liver biopsies. AN contributed to conduction and analysis of the HLA-class II coated bead assay and contributed to cholangiocyte organoid experiments. BP conducted and analysed the HLA-DP expression analysis on B cells. MEB contributed to cholangiocyte organoid experiments. YY and MM performed HLA-typing. DG designed and synthesised gRNA. JS-S performed immunohistochemistry experiments. JN, SB, LMM, RH, PK, TF and JD contributed to acquisition and processing of liver samples and generation of cholangiocyte organoids. MW, TP, MS, KJO and GS contributed to the establishment of patient cohorts and sample collection. IPSCSG served as collaborator for the genetic studies. EE, FD and AF contributed to analysis and interpretation of the genetic data. BF supervised design and synthesis of gRNA. US supervised immunohistochemistry experiments. CK, AH, MC and MJB participated in data analysis and gave critical intellectual input. SC contributed to data analysis and supervision of the study. MA designed and supervised the study. BFZ wrote the first draft of the manuscript. SC and MA revised and edited the manuscript. MA serves as guarantor for the study. All authors revised the manuscript and approved it for publication.

Funding BFZ, MA and CS (project number 290522633) were supported by the CRU 306 Primary sclerosing cholangitis. This project has received funding from the European Research Council (ERC) under the European Union's Horizon 2020 research and innovation programme (grant agreement no 884830). The project received funding from the DFG (Deutsche Forschungsgemeinschaft) grant no. EL 831/7-1 (project number 507145175), SFB841/SP2 and infrastructure support from the DFG Cluster of Excellence 2167 'Precision Medicine in Chronic Inflammation (PMI)' (EXC 2167-390884018). AH was supported by the Federal Ministry of Education and Research (01KI2110). CS, SB and JN were supported by the Landesforschungsförderung Hamburg (LFF-FV78). MEB was supported by the Daisy Hüet Roel Foundation (DHRF). This project has been funded in whole or in part with federal funds from the Frederick National Laboratory for Cancer Research, under Contract No. HHSN261200800001E. This Research was supported in part by the Intramural Research Program of the NIH, Frederick National Lab, Center for Cancer Research.

Disclaimer The content of this publication does not necessarily reflect the views or policies of the Department of Health and Human Services, nor does mention of trade names, commercial products, or organisations imply endorsement by the US Government.

Competing interests None declared.

Patient and public involvement Patients and/or the public were not involved in the design, or conduct, or reporting, or dissemination plans of this research.

Patient consent for publication Not applicable.

Ethics approval This study involves human participants and was approved by Ethics Commitee Landesärztekammer Hamburg (PV4780, PV4081, PV4898 and PV5184). Participants gave informed consent to participate in the study before taking part.

Provenance and peer review Not commissioned; externally peer reviewed.

Data availability statement Data are available on reasonable request.

ORCID iDs
Britta F Zecher http://orcid.org/0000-0001-7248-7266
David Ellinghaus http://orcid.org/0000-0002-4332-6110
Boris Fehse http://orcid.org/0000-0001-9780-7211
Marcus Altfeld http://orcid.org/0000-0001-5972-2997

REFERENCES

1 Trivedi PJ, Hirschfield GM. Recent advances in clinical practice: epidemiology of autoimmune liver diseases. *Gut* 2021;70:1989–2003.
2 Thorpe ME, Scheuer PJ, Sherlock S. Primary Sclerosing cholangitis, the biliary tree, and ulcerative colitis. *Gut* 1967;8:435–48.
3 Karlsen TH, Folseraas T, Thorburn D, *et al*. Primary sclerosing cholangitis - a comprehensive review. *J Hepatol* 2017;67:1298–323.
4 Visseren T, Erler NS, Heimbach JK, *et al*. Inflammatory conditions play a role in recurrence of PSC after liver transplantation: an international Multicentre study. *JHEP Rep* 2022;4:100599.
5 Jiang X, Karlsen TH. Genetics of primary Sclerosing cholangitis and pathophysiological implications. *Nat Rev Gastroenterol Hepatol* 2017;14:279–95.
6 Karlsen TH, Franke A, Melum E, *et al*. Genome-wide association analysis in primary sclerosing cholangitis. *Gastroenterology* 2010;138:1102–11.
7 Melum E, Franke A, Schramm C, *et al*. Genome-wide association analysis in primary sclerosing cholangitis identifies two non-HLA susceptibility Loci. *Nat Genet* 2011;43:17–9.
8 Spurkland A, Saarinen S, Boberg KM, *et al*. HLA class II Haplotypes in primary sclerosing cholangitis patients from five European populations. *Tissue Antigens* 1999;53:459–69.
9 Underhill JA, Donaldson PT, Doherty DG, *et al*. HLA DPB polymorphism in primary sclerosing cholangitis and primary biliary cirrhosis. *Hepatology* 1995;21:959–62.
10 Ravichandran G, Neumann K, Berkhout LK, *et al*. Interferon-Γ-dependent immune responses contribute to the pathogenesis of sclerosing cholangitis in mice. *J Hepatol* 2019;71:773–82.
11 Stiglund N, Strand K, Cornillet M, *et al*. Retained NK cell phenotype and Functionality in non-alcoholic fatty liver disease. *Front Immunol* 2019;10:1255.
12 Krämer B, Nalin AP, Ma F, *et al*. Single-cell RNA sequencing identifies a population of human liver-type Ilc1S. *Cell Rep* 2023;42:111937.
13 Waggoner SN, Cornberg M, Selin LK, *et al*. Natural killer cells act as Rheostats Modulating antiviral T cells. *Nature* 2011;481:394–8.
14 Textor S, Fiegler N, Arnold A, *et al*. Human NK cells are alerted to induction of P53 in cancer cells by upregulation of the Nkg2D ligands Ulbp1 and Ulbp2. *Cancer Res* 2011;71:5998–6009.
15 Barrow AD, Edeling MA, Trifonov V, *et al*. Natural killer cells control tumor growth by sensing a growth factor. *Cell* 2018;172:534–48.
16 Arnon TI, Lev M, Katz G, *et al*. Recognition of viral hemagglutinins by Nkp44 but not by Nkp30. *Eur J Immunol* 2001;31:2680–9.
17 Hershkovitz O, Jivov S, Bloushtain N, *et al*. Characterization of the recognition of tumor cells by the natural cytotoxicity receptor, Nkp44. *Biochemistry* 2007;46:7426–36.
18 Niehrs A, Garcia-Beltran WF, Norman PJ, *et al*. A subset of HLA-DP molecules serve as ligands for the natural cytotoxicity receptor Nkp44. *Nat Immunol* 2019;20:1129–37.
19 Steimle V, Siegrist CA, Mottet A, *et al*. Regulation of MHC class II expression by interferon-gamma mediated by the Transactivator gene CIITA. *Science* 1994;265:106–9.
20 Otten LA, Steimle V, Bontron S, *et al*. Quantitative control of MHC class II expression by the Transactivator CIITA. *Eur J Immunol* 1998;28:473–8.
21 Herkel J, Jagemann B, Wiegard C, *et al*. MHC class II-expressing hepatocytes function as antigen-presenting cells and activate specific Cd4 T lymphocytes. *Hepatology* 2003;37:1079–85.
22 Büning J, Hundorfean G, Schmitz M, *et al*. Antigen targeting to MHC class II-enriched late endosomes in Colonic epithelial cells: trafficking of luminal antigens studied in vivo in crohn's colitis patients. *FASEB J* 2006;20:359–61.
23 Salzberger W, Martrus G, Bachmann K, *et al*. Tissue-resident NK cells differ in their expression profile of the nutrient transporters Glut1, Cd98 and Cd71. *PLoS One* 2018;13:e0201170.
24 Ellinghaus D, Jostins L, Spain SL, *et al*. Analysis of five chronic inflammatory diseases identifies 27 new associations and highlights disease-specific patterns at shared Loci. *Nat Genet* 2016;48:510–8.
25 Delaneau O, Zagury J-F, Marchini J. Improved whole-Chromosome phasing for disease and population genetic studies. *Nat Methods* 2013;10:5–6.
26 Browning BL, Browning SR. Genotype imputation with millions of reference samples. *Am J Hum Genet* 2016;98:116–26.
27 Zheng X, Shen J, Cox C, *et al*. HIBAG--HLA genotype imputation with attribute bagging. *Pharmacogenomics J* 2014;14:192–200.
28 Degenhardt F, Wendorff M, Wittig M, *et al*. Construction and benchmarking of a multi-ethnic reference panel for the imputation of HLA class I and II Alleles. *Hum Mol Genet* 2019;28:2078–92.
29 Abraham G, Qiu Y, Inouye M. Flashpca2: principal component analysis of biobank-scale genotype datasets. *Bioinformatics* 2017;33:2776–8.
30 Broutier L, Andersson-Rolf A, Hindley CJ, *et al*. Culture and establishment of self-renewing human and Mouse adult liver and pancreas 3d organoids and their genetic manipulation. *Nat Protoc* 2016;11:1724–43.
31 Dekkers JF, Alieva M, Wellens LM, *et al*. High-resolution 3d imaging of fixed and cleared organoids. *Nat Protoc* 2019;14:1756–71.
32 Liaskou E, Jeffery LE, Trivedi PJ, *et al*. Loss of Cd28 expression by liver-infiltrating T cells contributes to pathogenesis of primary sclerosing cholangitis. *Gastroenterology* 2014;147:221–32.
33 Van Den Heuvel MC, Slooff MJ, Visser L, *et al*. Expression of anti-Ov6 antibody and anti-N-CAM antibody along the biliary line of normal and diseased human livers. *Hepatology* 2001;33:1387–93.
34 Hudspeth K, Donadon M, Cimino M, *et al*. Human liver-resident Cd56(Bright)/Cd16(Neg) NK cells are retained within hepatic sinusoids via the engagement of Ccr5 and Cxcr6 pathways. *J Autoimmun* 2016;66:40–50.
35 Borrego F, Peña J, Solana R. Regulation of Cd69 expression on human natural killer cells: differential involvement of protein kinase C and protein tyrosine Kinases. *Eur J Immunol* 1993;23:1039–43.
36 Hollenbach JA, Madbouly A, Gragert L, *et al*. A combined Dpa1∼Dpb1 amino acid EPITOPE is the primary unit of selection on the HLA-DP Heterodimer. *Immunogenetics* 2012;64:559–69.
37 Schöne B, Bergmann S, Lang K, *et al*. Predicting an HLA-Dpb1 expression marker based on standard Dpb1 Genotyping: linkage analysis of over 32,000 samples. *Hum Immunol* 2018;79:20–7.
38 Thomas R, Thio CL, Apps R, *et al*. A novel variant marking HLA-DP expression levels predicts recovery from hepatitis B virus infection. *J Virol* 2012;86:6979–85.
39 Quatrini L, Molfetta R, Zitti B, *et al*. Ubiquitin-dependent Endocytosis of Nkg2D-Dap10 receptor complexes activates signaling and functions in human NK cells. *Sci Signal* 2015;8:ra108.
40 Dyson JK, Beuers U, Jones DEJ, *et al*. Primary Sclerosing cholangitis. *The Lancet* 2018;391:2547–59.
41 Kambayashi T, Laufer TM. Atypical MHC class II-expressing antigen-presenting cells: can anything replace a Dendritic cell *Nat Rev Immunol* 2014;14:719–30.
42 Klitz W, Stephens JC, Grote M, *et al*. Discordant patterns of linkage disequilibrium of the peptide-transporter Loci within the HLA class II region. *Am J Hum Genet* 1995;57:1436–44.
43 Petersdorf EW, Malkki M, O'hUigin C, *et al*. High HLA-DP expression and graft-versus-host disease. *N Engl J Med* 2015;373:599–609.
44 Yamazaki T, Umemura T, Joshita S, *et al*. A cis-eQTL of HLA-Dpb1 affects susceptibility to type 1 autoimmune hepatitis. *Sci Rep* 2018;8:11924.
45 Kamatani Y, Wattanapokayakit S, Ochi H, *et al*. A genome-wide Association study identifies variants in the HLA-DP locus associated with chronic hepatitis B in Asians. *Nat Genet* 2009;41:591–5.
46 Adam R, Karam V, Delvart V, *et al*. Evolution of indications and results of liver transplantation in Europe. A report from the European liver transplant Registry (ELTR). *J Hepatol* 2012;57:675–88.
47 Aoki C, Bowlus C, Gershwin M. The Immunobiology of primary Sclerosing cholangitis. *Autoimmunity Reviews* 2005;4:137–43.
48 Katt J, Schwinge D, Schoknecht T, *et al*. Increased T helper type 17 response to pathogen stimulation in patients with primary Sclerosing cholangitis. *Hepatology* 2013;58:1084–93.
49 Bozward AG, Ronca V, Osei-Bordom D, *et al*. Gut-liver immune traffic: Deciphering immune-pathogenesis to underpin Translational therapy. *Front Immunol* 2021;12:711217.
50 Fasbender F, Widera A, Hengstler JG, *et al*. Natural killer cells and liver fibrosis. *Front Immunol* 2016;7:19.
51 Langeneckert AE, Lunemann S, Martrus G, *et al*. Ccl21-expression and accumulation of Ccr7+ NK cells in livers of patients with primary Sclerosing cholangitis. *Eur J Immunol* 2019;49:758–69.
52 Harmon C, Robinson MW, Fahey R, *et al*. Tissue-resident Eomes(Hi) T-Bet(Lo) Cd56(Bright) NK cells with reduced proinflammatory potential are enriched in the adult human liver. *Eur J Immunol* 2016;46:2111–20.
53 Broomé U, Glaumann H, Hultcrantz R, *et al*. HLA-DQ antigens in liver tissue from patients with primary sclerosing cholangitis. *Scand J Gastroenterol* 1990;25:54–8.
54 Cruickshank SM, Southgate J, Selby PJ, *et al*. Expression and cytokine regulation of immune recognition elements by normal human biliary epithelial and established liver cell lines in vitro. *J Hepatol* 1998;29:550–8.
55 Schrumpf E, Tan C, Karlsen TH, *et al*. The biliary epithelium presents antigens to and activates natural killer T cells. *Hepatology* 2015;62:1249–59.

56 Banales JM, Huebert RC, Karlsen T, *et al*. Cholangiocyte pathobiology. *Nat Rev Gastroenterol Hepatol* 2019;16:269–81.
57 Jalan-Sakrikar N, Brevini T, Huebert RC, *et al*. Organoids and regenerative hepatology. *Hepatology* 2023;77:305–22.
58 Fiorotto R, Amenduni M, Mariotti V, *et al*. Liver diseases in the dish: iPSC and Organoids as a new approach to modeling liver diseases. *Biochim Biophys Acta Mol Basis Dis* 2019;1865:920–8.
59 Brevini T, Maes M, Webb GJ, *et al*. FXR inhibition may protect from SARS-Cov-2 infection by reducing Ace2. *Nature* 2023;615:134–42.
60 Hoorweg K, Peters CP, Cornelissen F, *et al*. Functional differences between human Nkp44(-) and Nkp44(+) RORC(+) innate Lymphoid cells. *Front Immunol* 2012;3:72.
61 Cella M, Fuchs A, Vermi W, *et al*. A human natural killer cell subset provides an innate source of IL-22 for Mucosal immunity. *Nature* 2009;457:722–5.
62 Glatzer T, Killig M, Meisig J, *et al*. RORγt^{+} innate Lymphoid cells acquire a proinflammatory program upon engagement of the activating receptor Nkp44. *Immunity* 2013;38:1223–35.
63 Baumdick ME, Niehrs A, Degenhardt F, *et al*. HLA-DP on epithelial cells enables tissue damage by Nkp44^{+} natural killer cells in ulcerative colitis. *Gastroenterology* 2023.